Microsaccades drive illusory motion in the *Enigma* illusion

Xoana G. Troncoso*, Stephen L. Macknik*, Jorge Otero-Millan*†, and Susana Martinez-Conde*‡

*Barrow Neurological Institute, 350 West Thomas Road, Phoenix, AZ 85013; and †University of Vigo, Campus Universitario Lagoas-Marcosende, 36200 Vigo, Spain

Edited by Ranulfo Romo, Universidad Nacional Autónoma de México, Mexico City, Mexico, and approved August 6, 2008 (received for review October 2, 2007)

Visual images consisting of repetitive patterns can elicit striking illusory motion percepts. For almost 200 years, artists, psychologists, and neuroscientists have debated whether this type of illusion originates in the eye or in the brain. For more than a decade, the controversy has centered on the powerful illusory motion perceived in the painting *Enigma*, created by op-artist Isia Leviant. However, no previous study has directly correlated the *Enigma* illusion to any specific physiological mechanism, and so the debate rages on. Here, we show that microsaccades, a type of miniature eye movement produced during visual fixation, can drive illusory motion in *Enigma*. We asked subjects to indicate when illusory motion sped up or slowed down during the observation of *Enigma* while we simultaneously recorded their eye movements with high precision. Before ''faster'' motion periods, the rate of microsaccades increased. Before ''slower/no'' motion periods, the rate of microsaccades decreased. These results reveal a direct link between microsaccade production and the perception of illusory motion in *Enigma* and rule out the hypothesis that the origin of the illusion is purely cortical.

bistable perception | fixational eye movements | miniature eye movements | subjective motion | visual fixation

Isia Leviant's *Enigma* is one of the most famous examples of kinetic op-art (1). This static image (Fig. 1*A*) elicits powerful illusory motion in most observers and has generated an enormous amount of interest in the visual sciences since its creation in 1981. However, the origin of the illusion—the brain; the eye; or, possibly, a combination of both—remains, appropriately, an enigma. Here, we demonstrate directly that small saccades can drive the perception of illusory motion in *Enigma*. Our results are compatible with a causal relationship between increased microsaccade rates and the perception of illusory motion.

The "trickling" motion that can be seen within *Enigma*'s rings was serendipitously observed by MacKay on the wallboard of a BBC studio–the broadcasting staff had been annoyed by illusory shadows running up and down blank strips between columns of parallel lines (2). The illusion was later optimized by Leviant in the now classic *Enigma* design (1, 3), and it continues to inspire novel variants (4). Simpler patterns of regular stimuli, such as radial lines (i.e., MacKay "rays") or concentric rings, may also induce illusory motion at right angles to those of the stimulus pattern (2, 5) [supporting information (SI) Fig. S1*A*].

Three main types of mechanism have been proposed to explain this illusion. One possibility is that normal rapid fluctuations in the accommodation of the eye give rise to changes in the retinal image and thus to retinal signals. The origins of this hypothesis date back almost 200 years to Helmholtz (6) and Purkinje (7, 8), although the main arguments were later developed by Campbell and Robson (9), Millodot (10), and Gregory (11). If this idea is correct, then illusory motion from static patterns arises because of the optics of the eye. A second hypothesis was proposed by MacKay, who suggested that the illusory motion was the sole product of brain processes (2, 9). This hypothesis was later supported by Zeki *et al.* (12), who found different sets of cortical areas to be active during the perception of objective vs. illusory motion, and more recently by Kumar and Glaser (13) and Hamburger (14). The third potential explanation of illusory motion in static repetitive patterns came from Pritchard (15), who proposed that the illusion might be due to changes in retinal stimulation produced by small eye movements. This proposal was supported by Evans and Marsden (16), Mon-Williams and Wann (17), and Zanker and colleagues (18–20), who investigated another op-art painting giving rise to illusory motion effects: *Fall*, by Bridget Riley (Fig. S1*B*).

Historically, the research on illusory motion from static patterns has generated several notorious debates. For instance, the role of eye movements was ruled out very early in the process: MacKay noted that the illusory motion remained present under conditions of retinal stabilization, in which eye movements were nullified (21). However, Evans and Marsden (16) claimed that MacKay's retinal stabilization results were inconclusive because of limitations in his contact lens-based stabilization technique [such as significant slip of the contact lens over the scleral surface (22)]. To achieve perfect retinal stabilization, Evans and Marsden induced a prolonged after-image by presenting a very brief, intense illumination flash of the stimulus pattern. Because the illusory motion was absent in the resultant after-image, Evans and Marsden concluded that eye movements drove the effect. This conclusion was contested by Millodot (10), who pointed out that prolonged after-images eliminate both the effect of involuntary eye movements and the effect of accommodation fluctuations. Millodot argued that MacKay's stabilization results (2) ruled out eye movements as a contributor, and so later debate focused on the roles of accommodation vs. brain-generation of the *Enigma* illusion. However, if MacKay's stabilization technique was imprecise [as argued by Evans and Marsden (16)], then Millodot's reasoning was circular and eye movements should not have been ruled out. Nevertheless, the eye movement hypothesis was indeed set aside. Our current study aimed to test whether the eye movement hypothesis was ruled out prematurely.

The accommodation vs. brain construct debate continued. The two sides were championed by Gregory (11, 24, 26) and Zeki after the publication of Zeki and colleagues' imaging study in 1993 (12, 23, 25). However, no definitive conclusion was reached (see *Discussion* for further details). We note, however, that no studies to date have measured direct and tightly timed correlations between the subjective perception of illusory motion and the proposed physiological precursor.

Here, we set out to correlate microsaccades directly to the perception of illusory motion in *Enigma*. Microsaccades are small-

Author contributions: X.G.T., S.L.M., J.O.M., and S.M.-C. designed research; X.G.T. performed research; X.G.T., S.L.M., J.O.-M., and S.M.-C. analyzed data; and X.G.T., S.L.M., J.O.M., and S.M.-C. wrote the paper.

The authors declare no conflict of interest.

This article is a PNAS Direct Submission.

‡To whom correspondence should be addressed. E-mail: smart@neuralcorrelate.com.

This article contains supporting information online at www.pnas.org/cgi/content/full/0709389105/DCSupplemental.

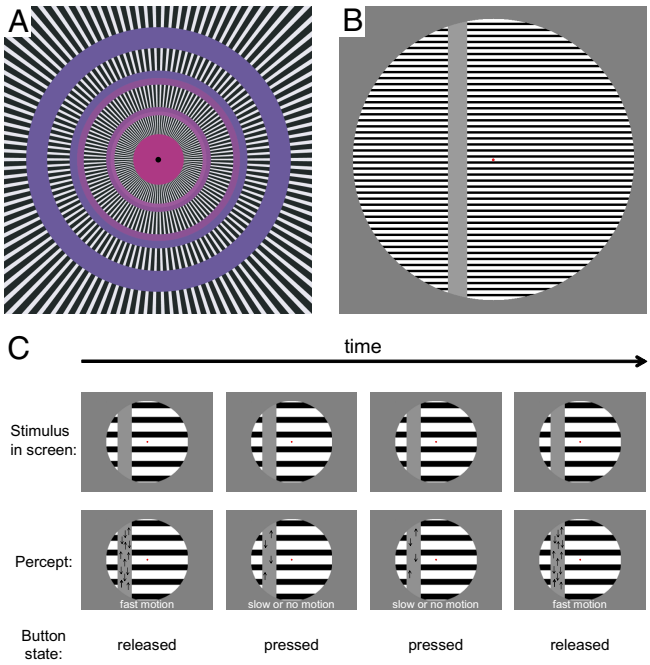

Fig. 1. Illusory motion in *Enigma*. (*A*) *Enigma* (1, 3). As one views the image the concentric purple annuli fill with rapid illusory motion. Upon careful fixation, the perception of illusory motion decreases or even stops completely. Subsequent eye movements bring back the illusory percept. (*B*) Simplified version of *Enigma* used in the present experiments (spatial characteristics slightly modified from those used in the actual experiments, for clarity). Illusory motion is seen to travel lengthwise along the gray stripe. (*C*) An epoch from a trial during the experiment. (*Top*) Schematic representation of the stimulus, which does not change over time. (*Middle*) Perception of the stimulus: the gray target stripe intermittently fills with fast or slow illusory motion. (*Bottom*) Subjects' report of their perception.

magnitude involuntary saccades that occur during fixation (27–29). These small eye movements generate strong neural transients in the early visual system (27, 30, 31), counteract visual fading during fixation (32) and prevent filling-in of artificial scotomas (33). Microsaccades may also play an important role on binocular rivalry (34). Van Dam and Van Ee recently found a clear correlation between microsaccadic retinal image changes and perceptual alternations during binocular rivalry (35). Our hypothesis, that microsaccades drive illusory motion in static patterns such as *Enigma*, was partly based on our own observations that the strength of illusory motion in *Enigma* is not stable across time, but that it varies as a function of how precisely one fixates. If one holds one's eyes still while viewing *Enigma*—for instance, by staring very carefully at the center of the image—one senses that the illusory motion decreases and occasionally comes to a full stop. Loose fixation qualitatively results in "faster" illusory motion. Previous research has shown that strict fixation suppresses the production of microsaccades, with dramatic effects on stimulus visibility (32, 33). It follows that, under normal (loose) fixation conditions, microsaccades may drive the perception of illusory motion in *Enigma* (27). Our results show a strong quantitative link between microsaccades and the perception of the *Enigma* illusion.

Results

Main Experiment: Perception of Illusory Motion in *Enigma*. Subjects were asked to fixate a small spot while viewing a simplified version of the *Enigma* illusion (Fig. 1*B*). They continuously reported (via button press) whether the perceived speed of motion was increasing (button released) or decreasing/no motion (button pressed). Their eye movements were recorded simultaneously with high precision. Fig. 1*C* describes a typical epoch during a trial.

As with other bistable stimuli paradigms (32, 35–38), subjects reported that their perception oscillated between two alternating states (motion speeding up vs. motion slowing down/fully stopped). We identified microsaccades (Fig. S2 *B* and *C*) and correlated them to the subject's perception, indicated via button press, at every point in time. The data show a clear positive relationship between increased microsaccade rates and the perception of "faster motion." Before transitions to a faster motion period, microsaccade rates increased (Fig. 2*A*, red line). Conversely, before transitions to a "slower/no" motion period, microsaccade rates decreased (Fig. 2*A*, blue line). The results were statistically significant (one-tailed paired t tests; $P < 0.05$; Fig. S3). These findings reveal a direct quantitative link between microsaccades and the perception of illusory motion.

To further establish the potential role of microsaccades in driving the *Enigma* illusion, we calculated the average probability of transitions to faster motion vs. slower/no motion percepts after microsaccade onsets (Fig. 2*B*). The data show that microsaccade onsets are followed by an increased probability of transitions to faster motion and a decreased probability of transitions to slower/no motion periods (a 172% peak increase and a 66% peak decrease from random, respectively). This suggests a causal relationship between microsaccades and transitions in illusory motion speed in *Enigma*. At the very least, we cannot exclude a causal role of microsaccades in driving the *Enigma* illusion, and specifically the perceptual transitions that characterize it.

Equivalent results were obtained when microsaccades were identified with a different algorithm (27, 30, 32, 39, 40), or when the maximum microsaccade magnitude threshold was set to 1°, 2° or 3° (Fig. S4). Equivalent results were also found in naïve and nonnaïve subjects (Fig. S5 *A* and B). Fig. S5*A* illustrates the large differences in peak-to-trough microsaccade rates for each subject (154%, 627%, and 910% from left to right). These percentage differences reflect the maximum microsaccade rates before transitions to faster motion over the minimum microsaccade rates before transitions to slower/no motion.

Control Experiment: Perception of Physical Changes in Motion Speed. We tested an alternative interpretation: that microsaccades do not drive the *Enigma* illusion and that *Enigma* instead causes both the perceptual report (button press/release) and the changes in microsaccade rates. If this were true, changes in microsaccade rates might precede the subjects' report (button press/release), as shown in Fig. 2*A*, but they would not precede the perceptual transitions. To test this possibility, we conducted a control experiment in which the same subjects indicated physical transitions in speed of motion, for real moving objects that simulated the *Enigma* illusion. The time delay (latency) between the physical transitions and the reported transitions in the control experiment was then used to estimate the timing between the perceptual transitions and the reported transitions in the main experiment (illusory motion condition) (35, 37, 38).

Subjects were asked to fixate on the center of the screen while viewing the same pattern as in the main experiment (Fig. 1*B*), but now with physical stimuli (small blobs) that moved up or down with increasing or decreasing speeds (see *Methods* for details). As in the main experiment, subjects continuously indicated changes in speed of motion by releasing (faster motion) or pressing (slower/no motion) a button while their eye movements were recorded. Subjects performed this task accurately; they correctly indicated 88 ± 1% of the transitions in speed of motion with an average latency of 520 ms (SD = 190 ms) (Fig. 2*C*). The average latency and SD values were consistent with those reported in refs. 35, 38, and 41 for various bistable stimuli.

Next, we calculated the rates of microsaccades around both the physical transitions (Fig. 2*D*) and the reported transitions (Fig. 2*E*)

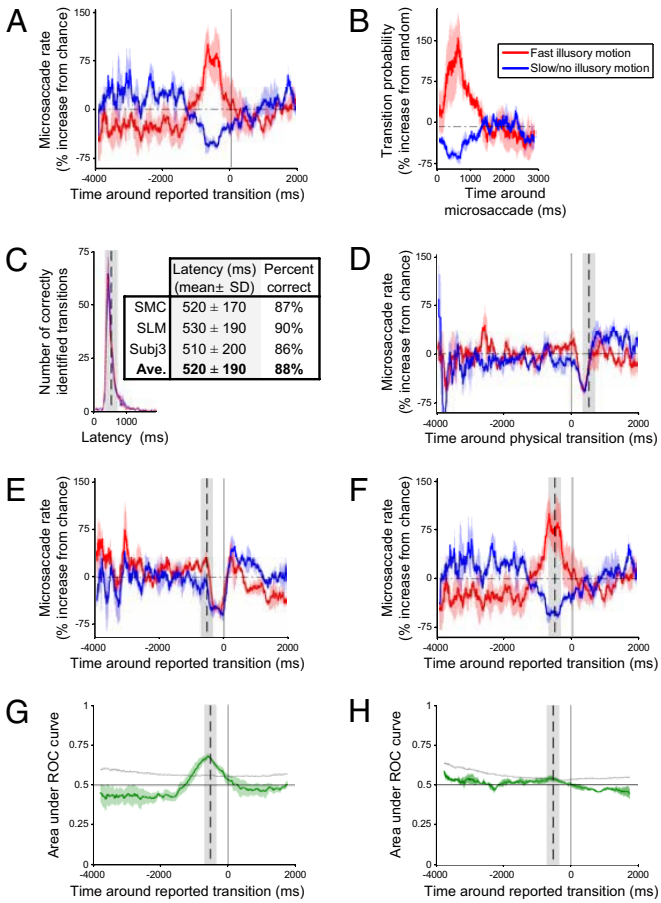

Fig. 2. Microsaccades can drive the perception of illusory motion in *Enigma*. (*A* and *B*) Perceptual transitions are correlated with previous microsaccades. (*A*) Average microsaccade rates around reported transitions toward faster (red) vs. slower/no (blue) illusory motion. (*B*) Average probability of transitions after microsaccade onset. The results are expressed as the percentage increase over a correlation where microsaccades happened at random times. Color code as in *A*. (*C–E*) Changes in microsaccade rates are not triggered by the perceptual transitions. Color code as in *A*. (*C*) Distribution of latencies from correctly identified physical transitions to reported transitions (control experiment). Dashed vertical line and surrounding gray band: average latency and standard deviation (SD) for all subjects (520 ± 190 ms). (*Inset*) Latency and performance parameters for individual subjects. (*D*) Average microsaccade rates around physical transitions in motion speed. Microsaccade rates decreased after both increases and decreases in physical motion speed. The vertical gray band indicates the estimated moment of the reported transitions with respect to the physical transitions (mean latency and SD from *C*). (*E*) Average microsaccade rates around reported transitions in nonillusory motion speed. The same data as in *D* are now realigned to the time of the subjects' report. The vertical gray band indicates the estimated moment of the physical transitions with respect to the reported transitions (from *C*). (*F*) Microsaccade rates around reported transitions in *Enigma*. Shown is the same graph as in *A*, now indicating the estimated moment of the perceived (illusory) transitions (vertical gray band; extrapolated from *C*). Microsaccade rates depart from baseline ≈740 ms before the time of the perceived transitions. (*G* and *H*) ROC analysis. The ideal observer can predict the type of illusory transition in *Enigma* (faster vs. slower/no motion) based on microsaccade rate. (*G*) The ideal observer's prediction (green line) becomes significantly better than chance ≈1,060 ms before the reported transitions (i.e., ≈540 ms before the perceptual transitions; estimated time of perceptual transitions indicated by vertical gray band). Horizontal dashed line indicates chance level (probability = 0.5). Thin gray line indicates the significance level, the level at which the ideal observer performs above chance with $P < 0.01$ (determined by permutation analysis, see *SI Methods* for details). Significance is reached whenever the green line is above the gray line. (*H*) The ideal observer cannot predict the type of transition in motion speed (faster vs. slower/no motion) for nonillusory moving objects. Other details are as in *G*. All of the panels show the average result for all subjects with the shaded red, blue and green areas indicating the SEM across subjects.

in motion speed (equivalent analyses as in Fig. 2*A*). Fig. 2*D* shows that the rate of microsaccades decreased after physical transitions in speed of motion, irrespective of whether the change in speed was toward faster or slower motion. This result is consistent with previous studies showing that changes in peripheral stimulation cause a transient drop in the rates of saccades and microsaccades, followed by a temporary enhancement (38, 42, 43). This transient course of "microsaccadic inhibition" may indicate a fast reflex of the oculomotor system to sudden changes in visual input (44). The vertical gray band in Fig. 2 *C* and *D* indicates the time of the reported transitions with respect to the physical transitions (latency: 520 ms ± 190 ms SD; calculated from Fig. 2*C*).

In Fig. 2*E*, the data from Fig. 2*D* have been realigned to the time of the button press/release, and the vertical gray band now indicates the time at which physical transitions occurred relative to the reported transitions (latency: −520 ms ± 190 ms SD). Note that the shape of the curve is similar to that in Fig. 2*D* (now shifted by the latency). Fig. 2 *D–E* show that faster stimulus motion is not preceded by increased microsaccade rates, as was found with the *Enigma* illusion (Fig. 2*A*). Rather, when subjects reported physical changes in motion (control experiment), microsaccade rates decreased after both increases and decreases in speed of motion (an ≈50% decrease in microsaccade rate, peaking ≈200 ms before the reported transition). This is contrary to our findings with illusory motion: microsaccade rates increased before transitions to faster motion and decreased before transitions to slower/no motion in *Enigma* (Fig. 2*A*). Thus, the perceptual transitions in *Enigma* do not drive changes in microsaccade rate. If microsaccade rate was driven by the percept of motion, then microsaccade rate would vary in the same way for both illusory motion (*Enigma* experiment) and physical motion (control experiment); however, it does not. Further, the control experiment provided us with the latency between perceptual transitions (caused by changes in physical motion) and reported transitions. This latency, when applied to the *Enigma* results, shows that changes in microsaccade rate precede the perception of the *Enigma* illusion. To determine this we overlaid the same gray band from Fig. 2 *C–E* (the time of the perceptual transition) on the data from the *Enigma* experiment (Fig. 2*A*). This analysis (Fig. 2*F*) illustrates that the perceptual transitions during *Enigma* took place 520 ms ± 190 ms (SD) before the reported transitions. Note that microsaccade rates began changing (i.e., departed from baseline) ≈740 ms before the perceptual transitions and 1,260 ms before the reported transitions. These values were consistent across individual subjects (Fig. S5*C*). Thus, microsaccades may potentially drive the perceptual transitions in illusory motion, but not the other way around.

To further quantify our conclusions, we conducted a receiver operating characteristic (ROC) analysis to calculate the ability of an ideal observer to predict the type of transition (to faster motion vs. slower/no motion) based on microsaccade rates (Fig. 2 *G* and *H*). In the main experiment (*Enigma* illusion) the ideal observer becomes significantly better than chance (determined by permutation analysis) ≈1,060 ms before the reported transitions (≈540 ms before the perceptual transitions, estimated from the latency correction, Fig. 2*G*). In the control experiment (physical motion) the ideal observer cannot distinguish between both types of transitions (faster motion vs. slower/no motion) from microsaccade rates alone (Fig. 2*H*). Data from individual subjects are shown in Fig. S5 *D* and *E*.

Discussion

The controversy about the source(s) of illusory motion in *Enigma* and other static repetitive patterns is almost 200 years old, dating back to Purkinje (7, 8). One reason the debate has persisted this long may have been that the perceptual transitions in these illusions take place very rapidly on a time-scale that is difficult to measure psychophysically. Microsaccades moreover occur up to several times per second (see ref. 29 for a review of

microsaccade parameters). Here, we overcame these limitations by employing an event-triggered paradigm in which subjects continually indicated the speed of illusory motion in real-time as it undulated during fixation, while we simultaneously measured microsaccade rates (32, 33).

Our results show a direct relationship between microsaccades and the perception of illusory motion in *Enigma*. Further, our data support the hypothesis that microsaccades drive the *Enigma* illusion, and not the other way around. Thus, microsaccades, directly or indirectly, are at least one possible cause of the *Enigma* effect.

Debate on the Role of Accommodation Fluctuations in *Enigma*. Our results indicate that microsaccades can trigger the *Enigma* illusion, thus ruling out the hypothesis that the origin of the illusion is solely cortical (3, 12–14, 21). However, they do not exclude the possibility that additional factors, such as accommodation fluctuations (9–11), may also contribute to the perception of illusory motion in *Enigma*.

During the 1990s, Gregory argued that accommodation fluctuations were the driving force behind the *Enigma* effect (11, 24, 26), whereas Zeki rejected the accommodation fluctuations hypothesis (12, 23, 25). To fully understand the debate on the role of accommodation in *Enigma*, we must first define the key concepts of "accommodation" and "accommodation fluctuations." "Accommodation" is the change of shape of the crystalline lens that occurs whenever we shift our gaze from a distant to a near visual target (see refs. 45 and 46 for reviews). This change in shape modifies the power of the lens; young adults can accommodate up to 15–20 Diopters. However, even when fixating a stationary target, the shape of the lens changes rapidly and continually ["accommodation fluctuations" (47–51)]. Accommodation fluctuations are small in amplitude (up to 0.5 Diopters, average 0.1 Diopters), and their temporal frequency spectrum has two main peaks, one ≈0.6 Hz and one ≈2 Hz (48–50, 52).

To address the role of accommodation fluctuations, Gregory and Zeki showed subjects the *Enigma* illusion through small artificial pupils (pinholes) that they claimed eliminated the effects of accommodation fluctuations (23, 26). The two groups reported contradictory results: According to Zeki, the illusion could be seen through the pinhole [and thus the percept was not caused by accommodation fluctuations (23)], whereas Gregory reported that the pinhole abolished the illusion (26). The logic underlying these experiments was problematic, however, because a pinhole does not optically mitigate accommodation fluctuations (51, 53, 54). Although a small pinhole will prevent large accommodative responses (such as those related to shifting one's gaze between objects located at different distances), it does not eliminate the accommodation fluctuations found during visual fixation. Specifically, pinholes larger than 2 mm have no effect on the fluctuations, whereas pinholes smaller than 2 mm increase the power and amplitude of the fluctuations (51, 53, 54). Zeki used both 1.6- and 2.2-mm pinholes (23), whereas Gregory used a 4-mm pinhole (26). Moreover, as pointed out by Mon-Williams and Wann (17), the 4-mm pinhole used by Gregory (26) was too big to prevent even large accommodative responses (51).

Despite the drawbacks of the pinhole experiments stated above, Zeki (25) later offered some compelling evidence against the role of accommodation fluctuations in *Enigma*. Patients who had their lenses surgically removed and replaced with artificial lenses (and thus had lost the mechanism for accommodation) nevertheless perceived illusory motion in *Enigma*. Further, patients with "aphakic eyes"—that is, patients lacking both natural and artificial lenses—also saw the illusion. Thus, current experimental evidence does not support the involvement of accommodation fluctuations in the perception of the *Enigma* illusion. Future experiments seeking to demonstrate the role of accommodation fluctuations in *Enigma* should provide direct and tightly timed measurements of accommodation fluctuations as a function of the perception of illusory motion.

Effect of Microsaccades in the Perception of Illusory Motion in *Enigma*. Our results directly confirm the hypothesis proposed by Pritchard (15), Mon-Williams and Wann (17), and Zanker and colleagues (18–20) that small eye movements can drive the perception of illusory motion in *Enigma* and other static patterns. Thus, our findings are compatible with a causal relationship between microsaccade rates and the perception of illusory motion. Whereas motion-sensitive neurons in the extrastriate dorsal areas surrounding V5 (the human equivalent of primate area MT) (12) may be responsible for the perception of all motion percepts, including illusory motion in *Enigma*, our results fail to support the hypothesis that the *Enigma* effect is purely cortical in origin (3, 9, 12–14, 21).

We should note that, during free visual exploration conditions, both microsaccades and large saccades may trigger the *Enigma* illusion. However, large saccades were essentially absent from our experiments, because subjects maintained visual fixation during the task. Future research should determine whether any other eye movements types, in addition to microsaccades (such as large saccades, tremor, and/or drifts), may also contribute to the *Enigma* illusion.

No other study, to our knowledge, has shown a direct and tightly timed link between microsaccades and the perception of illusory motion. Microsaccades may also be involved in the generation of illusory motion in other static patterns (39, 55), such as the MacKay rays (2), Bridget Riley's "Fall" (18, 19, 20), or the Ouchi illusion (56–58) (Fig. S1). Martinez-Conde (27) pointed out that many illusory motion effects are attenuated or even disappear altogether during careful fixation by the observer (which suppresses microsaccades). The present results are also consistent with predictions from physiological studies in which microsaccades were found to increase spiking rates in visual neurons in both the early visual system (27, 30, 31) and primate motion area MT (59).

Of central interest is the mechanism by which microsaccades may drive illusory motion in static patterns such as *Enigma*. Mon-Williams and Wann (17) proposed that small eye movements produce shifts in the geometrical position of the peripheral portions of the image. Such shifts result in continuous contrast reversals, thus generating phi movement—the illusion of apparent motion produced by switching off one stimulus and immediately turning on another one in close proximity (60). A nonmutually exclusive possibility is that microsaccades may displace after-images caused by the black and white stripes in the pattern and thus cause phi movement. Conway and coworkers (61, 63) recently showed that pairs of stimuli of different contrasts can generate motion signals (i.e., phi movement) in directionally selective neurons of areas V1 and MT, and proposed that this neural mechanism may underlie the perception of another type of illusory motion from static patterns (61–63). Whatever neural circuit is responsible for the percept, the link between microsaccades and the generation of illusory motion signals has not been directly demonstrated until now.

Materials and Methods

Subjects. Three subjects (two females, one male) with normal or corrected-to-normal vision participated in this study. Each subject participated in five sessions: one training session and four experimental sessions [two sessions in the main experiment (*Enigma* illusion) and two sessions in the control experiment (physical motion)] of ≈30 min each. One subject was naïve, and two subjects were authors in this article. An additional naïve subject was initially tested in the main experiment, with equivalent results (data not shown), but had to be removed from the final study because he was not available to participate in the control experiment. Due to the complexity of the task, all participating subjects were experienced in making observations during fixation tasks. Potential subjects who reported difficulties assessing the illusion during the training session were discarded. Naïve subjects were paid $15 per session. Experiments were carried out under the guidelines of the Barrow Neurological Institute's Institutional Review Board (protocol 04BN039), and written informed consent was obtained from each participant.

Eye Movements Recordings and Analyses. Eye position was acquired noninvasively with a fast video-based eye movement monitor (EyeLink II, SR Research).

The EyeLink II system records eye position simultaneously in both eyes (temporal resolution 500 samples per second; instrument noise 0.01° rms), in its off-the-shelf configuration.

We identified and removed blink periods as the portions of the EyeLink II recorded data where the pupil information was missing. We further added 200 ms before and after each period to also eliminate the initial and final parts of the blink, where the pupil is partially occluded. We moreover removed those portions of the data corresponding to very fast decreases and increases in pupil area (>20 units per sample) plus the 200 ms before and after. Such periods are probably due to partial blinks, where the pupil is never fully occluded (thus failing to be identified as a blink by EyeLink II) (33).

We identified microsaccades automatically with an objective algorithm (see ref. 43 for details) with a maximum microsaccade magnitude threshold of 2°. Equivalent results (event-triggered averages and ROC analyses) were found for 1° and 3° thresholds. To reduce the amount of potential noise (64), we analyzed only binocular microsaccades (that is, microsaccades with a minimum overlap of one data sample in both eyes) (33, 44, 64–66). Additionally, we imposed a minimum intersaccadic interval of 20 ms so that overshoot corrections were not categorized as microsaccades (33, 67). Fig. S2 *B* and C shows the main sequence of all analyzed microsaccades (n = 10,154 microsaccades) (68) and their direction distribution. More than 90% of all microsaccades were smaller than 1°. Table S1 summarizes the average microsaccade parameters for each subject.

Experimental Design. Subjects rested their head on a chin-rest 57 cm from a linearized video monitor (Barco Reference Calibrator V, 75-Hz refresh rate).

***Main experiment: Perception of illusory motion in* Enigma.** Subjects fixated on a small spot on the center of the monitor's screen and simultaneously reported the perceived speed of motion on a simplified version of the *Enigma* illusion (Fig. 1*B*) via button press. The fixation spot was a red dot (0.05° in diameter) placed on the center of the image. Subjects pressed a key, and a simplified version of the *Enigma* illusion (Fig. 1*B*), optimized to strengthen the illusory motion (3, 13), appeared on the screen.

The circle in Fig. 1*B* was 27.8° in diameter. Each of the parallel black lines was 0.24° wide and was separated from the lines above and below by a 0.36° gap. The gray band (1.90° wide) was placed at an eccentricity of 2.58° from the fixation spot. The luminance of the gray band (60% gray) matched the mean luminance of the stimulus. To avoid adaptation across trials, the whole image was randomly rotated toward one of eight chosen points around the compass (45°, 90°, 135°, 180°, 225°, 270°, 315°) from one trial to the next. This rotation did not affect the strength of the illusion (13).

Subjects were asked to press a button if the speed of motion within the gray band (Fig. 1*B*) decreased (or completely stopped) and to release the button if the speed of motion increased. The distribution of faster motion and slower/no motion periods for the average of all subjects is plotted in Fig. S2*A*, and the corresponding parameters summarized in Table S1.

After 30 s, all stimuli disappeared and the trial ended. To disregard the potential effect of the initial stimulus-onset transient at the start of each trial, we conducted analyses only on those data recorded after the first button press. Each experimental session included 40 trials.

Control experiment: Perception of physical changes in motion speed. We conducted a control experiment with the same *Enigma* pattern as in the main experiment above. However, we now introduced 120 small blobs moving up or down the gray stripe and changed their speed of motion according to the timing of the transitions reported by one of the subjects in the main experiment. The blobs were difference of gaussians filters (σ_{center} = 0.04°, $\sigma_{surround}$ = 0.08°) with the same mean luminance as the gray band (60% gray), moving at one of five possible speeds: 0, 2, 4, 8, and 16 deg/s. Such range of (non-zero) motion speeds is known to activate early visual system neurons (69). The first speed in each trial was randomly chosen from 2, 4, 8, or 16 deg/s. Then, we alternated between transitions to slower and faster speeds (the specific speed being again randomly assigned) according to the timing of the transitions reported by one of the subjects in the main experiment (*Enigma* illusion). All other details, including the subjects' task, were as in the main experiment.

We calculated the average latency between physical transitions in speed of motion and reported transitions (subjects' button presses/releases) (Fig. 2*C*). To do this, we disregarded latency values >1,500 ms [1% of all reported transitions; such latencies were considered too long to be meaningful (41)].

Event-Triggered Averages. Event-triggered averages (Fig. 2) were calculated by averaging a multisecond window of data around or after the trigger event (the reported transition in Fig. 2 *A*, *E*, and *F*; the microsaccade onset in Fig. 2*B*; or the physical transitions in Fig. 2*D*). Thus, the event-triggered average in Fig. 2*A* represents the average microsaccade rate at any given time during the 6-s window plotted around the reported transitions (all reported transitions are aligned at time 0 ms). If there were <6 s of data around a trigger event (due to the edge of the recording time during that specific trial), the 6-s window was dynamically reduced to fit the available data. For the analyses where the trigger event was a transition, we avoided using the same data point multiple times by considering only the time from the previous transition until the next transition (41).

Individual subjects' event-triggered averages concerning microsaccade rates and transition probabilities were calculated with a 150-ms sliding window that advanced one data sample (2 ms) each iteration. For each subject, calculations were made separately for each eye and then averaged between the two eyes. The population average and SEM were then calculated across subjects.

Probability of Perceptual Transitions Triggered by Microsaccade Onsets. Only microsaccades produced during a slower/no motion period may possibly trigger a transition to a period of faster motion. Conversely, only microsaccades produced during a period of faster motion may trigger a transition to a period of slower/no motion. Thus to calculate the probability of transitions to faster motion after microsaccade onsets, we only considered those microsaccades that were produced during the previous slower/no motion period (as determined by the subjects' reports). Likewise, to calculate the probability of transitions to slower/no motion after microsaccade onsets, we only considered those microsaccades that occurred during the previous faster motion period. To ensure that any results obtained would not be due to chance correlations between the dynamics of microsaccades and those of perceptual transitions, we repeated the above calculations, this time replacing microsaccades with the same number of events, now randomly distributed in time, for each subject. We then repeated this randomization by a factor equal to the number of microsaccades measured for each subject. We thus obtained a baseline for each subject, from which we calculated the percentage increase in the probability of perceptual transitions after actual microsaccades (Fig. 2*B*). This analysis is comparable with the ''cross-correlogram shuffling'' often used to rule out spurious correlations between potential presynaptic and postsynaptic neurons (70, 71).

ROC Analysis. We used a sliding receiver operating characteristic (ROC) analysis (72–77) to quantify how well microsaccade rate may predict the type of perceptual transition (faster motion vs. slower/no motion) in *Enigma*. The area under the ROC curve provides a measure of the discriminability of two signals and is directly related to the overlap of the two distributions of responses that are compared (74). In our case, the area under the ROC curve can be interpreted as the probability with which an ideal observer, given the microsaccade rate around a particular transition, can correctly determine the type of transition (faster motion vs. slower/no motion). An ROC area of 0.5 corresponds to completely overlapping distributions (the ideal observer cannot discriminate between the two types of transition); an area of 1 corresponds to transitions that can be perfectly discriminated based on microsaccade rate. This analysis makes no assumptions about the underlying distributions (74). For a given point in time, we compared the microsaccade rate distributions for faster motion (true-positive rate) and slower/no motion transitions (false-positive rate) in each subject. To obtain the ROC curve at that time, we plotted the probability of true positives as a function of the probability of false positives for all possible criterion response levels. We performed a sliding ROC analysis (kernel width 500 ms, slid in 2-ms increments) to calculate each subject's area under the ROC curve at each time point around the transition. To determine the time point at which the ideal observer became better than chance, we calculated significance, using a permutation procedure (74–78) with n = 1,000 shuffles for each subject and a criterion $P < 0.01$.

ACKNOWLEDGMENTS. We thank Dr. N Srivastava and M Stewart for technical assistance and H Rieiro for comments. This work was funded by the Barrow Neurological Foundation and National Science Foundation Award 0643306 (to S.M.-C.). X.G.T. is a Fellow of Caja Madrid Foundation.

1. Leviant I (1982) Illusory motion within still pictures: The L-effect. *Leonardo* 15:222–223.
2. MacKay DM (1957) Moving visual images produced by regular stationary patterns. *Nature* 180:489–490.
3. Leviant I (1996) Does ''brain power'' make Enigma spin? *Proc R Soc London Ser B* 263:997–1001.
4. Gori S, Hamburger K, Spillmann L (2006) Reversal of apparent rotation in the Enigma-figure with and without motion adaptation and the effect of T-junctions. *Vision Res* 46:3267–3273.
5. Spillmann L (1993) The perception of movement and depth in moire patterns. *Perception* 22:287–308.
6. Helmholtz H (1985) *Helmholtz's Treatise on Physiological Optics* (Gryphon Editions, Birmingham, Alabama).
7. Purkinje J (1823) *Beobachtungen und Versuche zur Physiologie der Sinne. Beitrage zur Kenntniss des Sehens in subjektiver Hinsicht Erstes Bandchen* (Calve, Prague).
8. Purkinje J (1825) *Beobachtungen und Versuche zur Physiologie der Sinne. Neue Beitrage zur Kenntniss des Sehens in subjektiver Hinsicht Zweites Bandchen* (Reimer, Berlin).

9. Pirenne MH, Campbell FW, Robson JG, MacKay DM (1958) Moving visual images produced by regular stationary patterns. *Nature* 181:362–363.
10. Millodot M (1968) Influence of accommodation on the viewing of an optical illusion. *Q J Exp Psychol* 20:329–335.
11. Gregory RL (1993) A comment: MacKay Rays shimmer due to accommodation changes. *Proc R Soc London Ser B* 253:123.
12. Zeki S, Watson JD, Frackowiak RS (1993) Going beyond the information given: The relation of illusory visual motion to brain activity. *Proc Biol Sci* 252:215–222.
13. Kumar T, Glaser DA (2006) Illusory motion in Enigma: A psychophysical investigation. *Proc Natl Acad Sci USA* 103:1947–1952.
14. Hamburger K (2007) Apparent rotation and jazzing in Leviant's Enigma illusion. *Perception* 36:797–807.
15. Pritchard R (1958) Visual illusions viewd as stabilized retinal images. *Q J Exp Psychol* 10:77–81.
16. Evans CR, Marsden RP (1966) A study of the effect of perfect retinal stabilization of some well-known visual illusions, using the after-image as a method of compensating for eye movements. *Br J Physiol Opt* 23:242–248.
17. Mon-Williams M, Wann JP (1996) An illusion that avoids focus. *Proc R Soc London Ser B* 263:573–578.
18. Zanker JM, Walker R (2004) A new look at Op art: Towards a simple explanation of illusory motion. *Naturwissenschaften* 91:149–156.
19. Zanker JM (2004) Looking at Op Art from a computational viewpoint. *Spat Vis* 17:75–94.
20. Zanker JM, Doyle M, Robin W (2003) Gaze stability of observers watching Op Art pictures. *Perception* 32:1037–1049.
21. MacKay DM (1957) Some further visual phenomena associated with regular patterned stimulation. *Nature* 180:1145–1146.
22. Barlow HB (1963) Slippage of contact lenses and other artifacts in relation to fading and regeneration of supposedly stable retinal images. *Q J Exp Psychol* 15:36–51.
23. Zeki S(1994) The cortical Enigma: A reply to Professor Gregory. *Proc Biol Sci* 257:243–245.
24. Gregory RL (1994) Under the carpet. *Perception* 23:741–744.
25. Zeki S (1995) Phenomenal motion seen through artificial intra-ocular lenses. *Proc Biol Sci* 260:165–166.
26. Gregory RL (1995) Brain-created visual motion: An illusion? *Proc R Soc London Ser B* 260:167–168.
27. Martinez-Conde S (2006) Fixational eye movements in normal and pathological vision. *Progress in Brain Res* 154:151–176.
28. Otero-Millan J, Troncoso XG, Macknik SL, Martinez-Conde S (2008) Saccades and microsaccades during visual fixation, exploration and search: foundations for a common saccadic generator. *J Vision*, in press.
29. Martinez-Conde S, Macknik SL, Hubel DH (2004) The role of fixational eye movements in visual perception. *Nat Rev Neurosci* 5:229–240.
30. Martinez-Conde S, Macknik SL, Hubel DH (2002) The function of bursts of spikes during visual fixation in the awake primate lateral geniculate nucleus and primary visual cortex. *Proc Natl Acad Sci USA* 99:13920–13925.
31. Martinez-Conde S, Macknik SL, Hubel DH (2000) Microsaccadic eye movements and firing of single cells in the striate cortex of macaque monkeys. *Nat Neurosci* 3:251–258.
32. Martinez-Conde S, Macknik SL, Troncoso XG, Dyar TA (2006) Microsaccades counteract visual fading during fixation. *Neuron* 49:297–305.
33. Troncoso XG, Macknik SL, Martinez-Conde S (2008) Microsaccades counteract perceptual filling-in. *J Vision*, in press.
34. Sabrin HW, Kertesz AE (1983) The effect of imposed fixational eye movements on binocular rivalry. *Percept Psychophys* 34:155–157.
35. van Dam LC, van Ee R (2006) Retinal image shifts, but not eye movements per se, cause alternations in awareness during binocular rivalry. *J Vis* 6:1172–1179.
36. Spillmann L, Kurtenbach A (1992) Dynamic noise backgrounds facilitate target fading. *Vision Res* 32:1941–1946.
37. van Dam LC, van Ee R (2005) The role of (micro)saccades and blinks in perceptual bi-stability from slant rivalry. *Vision Res* 45:2417–2435.
38. van Dam LC, van Ee R (2006) The role of saccades in exerting voluntary control in perceptual and binocular rivalry. *Vision Res* 46:787–799.
39. Macknik SL, Martinez-Conde S, Haglund MM (2000) The role of spatiotemporal edges in visibility and visual masking. *Proc Natl Acad Sci USA* 97:7556–7560.
40. Martinez-Conde S, Macknik SL (2007) Windows on the mind. *Sci Am* 297:56–63.
41. Einhauser W, Stout J, Koch C, Carter O (2008) Pupil dilation reflects perceptual selection and predicts subsequent stability in perceptual rivalry. *Proc Natl Acad Sci USA* 105:1704–1709.
42. Galfano G, Betta E, Turatto M (2004) Inhibition of return in microsaccades. *Exp Brain Res* 159:400–404.
43. Engbert R, Kliegl R (2003) Microsaccades uncover the orientation of covert attention. *Vision Res* 43:1035–1045.
44. Laubrock J, Engbert R, Kliegl R (2005) Microsaccade dynamics during covert attention. *Vision Res* 45:721–730.
45. Glasser, A (2006) Accommodation: Mechanism and measurement. *Ophthalmol Clin North Am* 19:1–12.
46. Mays LE, Gamlin, PD (1995) Neuronal circuitry controlling the near response. *Curr Opin Neurobiol* 5:763–768.
47. Alpern M (1958) Variability of accommodation during steady fixation at various levels of illuminance. *J Opt Soc Am* 48:193–197.
48. Campbell FW, Robson JG, Westheimer G (1959) Fluctuations of accommodation under steady viewing conditions. *J Physiol* 145:579–594.
49. Kotulak JC, Schor CM (1986) Temporal variations in accommodation during steady-state conditions. *J Opt Soc Am A* 3:223–227.
50. Winn B, Gilmartin B (1992) Current perspective on microfluctuations of accommodation. *Ophthalmic Physiol Opt* 12:252–256.
51. Gray LS, Winn B, Gilmartin B (1993) Effect of target luminance on microfluctuations of accommodation. *Ophthalmic Physiol Opt* 13:258–265.
52. Denieul P (1982) Effects of stimulus vergence on mean accommodation response, microfluctuations of accommodation and optical quality of the human eye. *Vision Res* 22:561–569.
53. Owens H, Baht K, Jacobs RJ (2004) Maxwellian and real pupils: Effect on accommodative microfluctuations. *Invest Ophthtalmol Visual* Sci 25:1280.
54. Stark LR, Atchison DA (1997) Pupil size, mean accommodation response and the fluctuations of accommodation. *Ophthalmic Physiol Opt* 17:316–323.
55. Fermuller C, Pless R, Aloimonos Y (1997) Families of stationary patterns producing illusory movement: Insights into the visual system. *Proc Biol Sci* 264:795–806.
56. Ouchi H (1977) *Japanese Optical and Geometrical Art* (Dover, New York).
57. Spillmann L, Tulunay-Keesey U, Olson J (1993) Apparent motion in normal and stabilised vision. *Invest Ophthalmol Visual Sci* 34:1031.
58. Pinna B, Spillmann L (2005) New illusions of sliding motion in depth. *Perception* 34:1441–1458.
59. Bair W, O'Keefe LP (1998) The influence of fixational eye movements on the response of neurons in area MT of the macaque. *Vis Neurosci* 15:779–786.
60. Wertheimer M (1923) Untersuchungen zur Lehre von der Gestalt, II. *Psychol Forsch* 4:301–350.
61. Conway BR, Kitaoka A, Yazdanbakhsh A, Pack CC, Livingstone MS (2005) Neural basis for a powerful static motion illusion. *J Neurosci* 25:5651–5656.
62. Livingstone MS, Pack CC, Born R (2001)T Two-dimensional substructure of MT receptive fields. *Neuron* 30:781–793.
63. Livingstone MS, Conway BR (2003) Substructure of direction-selective receptive fields in macaque V1. *J Neurophysiol* 89:2743–2759.
64. Engbert R (2006) Microsaccades: A microcosm for research on oculomotor control, attention, and visual perception. *Prog Brain Res* 154:177–192.
65. Engbert R, Mergenthaler K (2006) Microsaccades are triggered by low retinal image slip. *Proc Natl Acad Sci USA* 103:7192–7197.
66. Rolfs M, Laubrock J, Kliegl R (2006) Shortening and prolongation of saccade latencies following microsaccades. *Exp Brain Res* 169:369–376.
67. Moller F, Laursen ML, Tygesen J, Sjolie AK (2002) Binocular quantification and characterization of microsaccades. *Graefes Arch Clin Exp Ophthalmol* 240:765–770.
68. Zuber BL, Stark L (1965) Microsaccades and the velocity-amplitude relationship for saccadic eye movements. *Science* 150:1459–1460.
69. Martinez-Conde S, *et al.* (1999) Effects of feedback projections from area 18 layers 2/3 to area 17 layers 2/3 in the cat visual cortex. *J Neurophysiol* 82:2667–2675.
70. Martinez LM, Alonso JM (2001) Construction of complex receptive fields in cat primary visual cortex [see comments]. *Neuron* 32:515–525.
71. Alonso JM, Martinez LM (1998) Functional connectivity between simple cells and complex cells in cat striate cortex. *Nat Neurosci* 1:395–403.
72. Green DM, Swets JA (1966) *Signal Detection Theory and Psychophysics* (Wiley, New York).
73. Britten KH, Shadlen MN, Newsome WT, Movshon JA (1992) The analysis of visual motion: A comparison of neuronal and psychophysical performance. *J Neurosci* 12:4745–4765.
74. Feierstein CE, Quirk MC, Uchida N, Sosulski DL, Mainen ZF (2006) Representation of spatial goals in rat orbitofrontal cortex. *Neuron* 51:495–507.
75. Hernandez A, Zainos A, Romo R (2002) Temporal evolution of a decision-making process in medial premotor cortex. *Neuron* 33:959–972.
76. Romo R, Hernandez A, Zainos A (2004) Neuronal correlates of a perceptual decision in ventral premotor cortex. *Neuron* 41:165–173.
77. Romo R, Hernandez A, Zainos A, Lemus L, Brody CD (2002) Neuronal correlates of decision-making in secondary somatosensory cortex. *Nat Neurosci* 5:1217–1225.
78. Siegel S, Castellan NJ (1988) *Nonparametric Statistics for Behavioral Sciences* (McGraw-Hill, New York).